

Cosmological parameter estimation from CMB and X-ray clusters after Planck

Jian-Wei Hu,¹ Rong-Gen Cai,² Zong-Kuan Guo,³ Bin Hu⁴

^{1 2 3}State Key Laboratory of Theoretical Physics, Institute of Theoretical Physics, Chinese Academy of Sciences, P.O. Box 2735, Beijing 100190, China

⁴ Instituut-Lorentz for Theoretical Physics, Universiteit Leiden, 2333 CA Leiden, The Netherlands

Abstract. We update the cosmological parameter estimation for three non-vanilla models by a joint analysis of *CCCP* X-ray cluster, the newly released *Planck* CMB data as well as some external data sets, such as baryon acoustic oscillation measurements from the 6dFGS, SDSS DR7 and BOSS DR9 surveys, and Hubble Space Telescope H_0 measurement. First of all, we find that X-ray cluster data sets strongly favor a non-zero summed neutrino mass at more than 3σ confidence level in these non-vanilla models. And then, we reveal some tensions between X-ray cluster and *Planck* data in some cosmological parameters. For the matter power spectrum amplitude σ_8 , X-ray cluster data favor a lower value compared with *Planck*. Because of the strong $\sigma_8 - \sum m_\nu$ degeneracy, this tension could beyond 2σ confidence level when the summed neutrino mass $\sum m_\nu$ is allowed to vary. For the CMB lensing amplitude A_L , the addition of X-ray cluster data results in a 3σ deviation from the vanilla model. Furthermore, *Planck*+X-ray data prefer a large Hubble constant and phantom-like dark energy equation of state, which are in 2σ tension with those from WMAP7+X-ray data. Finally, we find that these tensions/descrepancies could be relaxed in some sense by adding a 9% systematic shift in the cluster mass functions.

Keywords: cosmology, neutrino mass, galaxy clusters

ArXiv ePrint: [0000.0000](https://arxiv.org/abs/0000.0000)

¹Email: jwhu@itp.ac.cn

²Email: cairg@itp.ac.cn

³Email: guozk@itp.ac.cn

⁴Email: hu@lorentz.leidenuniv.nl

Contents

1	Introduction	1
2	Data and methodology	2
3	Results	3
3.1	$\sum m_\nu$ results	4
3.2	A_L and σ_8 results	5
3.3	H_0 and w results	8
4	Conclusions	9

1 Introduction

Recently, the *Planck* Collaboration publicly released the initial cosmology products [1] based on the first 15.5 months of *Planck* operations. Their scientific results strongly support the standard 6-parameter Λ CDM model, hereafter namely the vanilla model. And the corresponding parameter constraints are greatly improved, including a highly significant deviation from scale invariance of the primordial power spectrum of curvature perturbations. However, some based cosmological parameter values and others derived from them are significantly different from those previously determined, such as present Hubble parameter H_0 [2], the lensing amplitude A_L [2], *etc.* Among these parameter estimation tensions, the most controversial one is about H_0 value. On the one hand, *Planck* results are discrepant with recent direct measurements from Hubble Space Telescope (HST) Key Project [3] and Type Ia supernovae observations via the magnitude-redshift relation, such as the Union2.1 compilation [4]. On the other hand, they are in excellent agreement with geometrical constraints from several baryon acoustic oscillation (BAO) surveys [5–7]. Beside that, very recently the authors of [39] re-analyze the *Planck* primary CMB data and find that the $217\text{ GHz} \times 217\text{ GHz}$ detector set spectrum used in the *Planck* analysis is responsible for some of this tension. In order to reveal or reconcile the tensions between low redshift geometric and *Planck* measurements, many efforts have been done [8–16].

Beside CMB observations, Large Scale Structure (LSS) surveys on various scales, such as galaxies and clusters of galaxies, could also provide us lots of cosmological information. A better understanding of the sturcture of our universe asks for the agreement between theoretical predictions and observations on various spatial and temporal scales. The cosmological information encoded in the CMB map is mainly on the spatially large scales and at temporally very deep redshift. As complementary observations, the distribution of LSS tells us the structure formation laws due to the instability of gravity on relatively small scales and at low redshifts. As the most massive virialised structures in the universe, clusters of galaxies are perfect probes of the matter distribution on large scales. Within the framework of dark matter structure formation scenario, baryonic matter traces the distribution of dark matter halo. When the baryonic gas falls into the gravitational potential wells, it could heat up to 10^7K so that X-rays will be emitted. Via this mechanism the galaxy clusters could be identified through their X-ray flux. *Chandra* Cluster Cosmology Project (*CCCP*) [17–20] utilizes X-rays indicator to observe the galaxy clusters that has been a catalog detected in a new

Rontgensatellite (Rosat) PSPC surveys [21] covering 400 square degrees sky area. Thanks to the high resolution of the *Chandra* X-rays observator, high-quality X-ray data of the resulting samples upto redshift $z = 0.9$ are obtained, which can be used to determine the galaxy cluster mass function and hence to estimate the cosmological parameters.

The detection of solar and atmospheric neutrino oscillations indicates that neutrinos are massive, but cannot provide absolute masses for neutrinos. Cosmological observations can provide significantly strong constraints on the summed neutrino mass through the cosmological effects of massive neutrinos. Neutrino masses affect the CMB power spectrum mainly through the early integrated Sachs-Wolfe effect, the BAO by changing the late-time expansion rate of the universe, and the abundance of galaxy clusters by smearing out a fraction of the mass over the neutrino free streaming scale [36]. The Planck team actually adopts a normal hierarchy for neutrino masses with $\sum m_\nu = 0.06$ eV as their baseline model and finds a significant discrepancy between the Planck data and the abundance of galaxy clusters [2]. This suggests that the tension is relaxed by increasing the summed neutrino mass because their free streaming reduces the amount of small scale clustering today. Therefore, in our analysis the summed neutrino mass is always allowed to be free. In this paper we focus on the cosmological parameter estimation for three non-vanilla models by using the *Planck*+WP+BAO+HST data in combination with *CCCP* X-ray clusters.

The rest parts of this paper are organized as follows. In Sec. 2 we will briefly describe the data sets and methodology. In Sec. 3 we will present our results in three non-vanilla models and reveal some tensions between X-ray cluster and *Planck* data. Finally we arrive at our conclusions in Sec. 4.

Table 1. List of cosmological parameters

Parameter	Range	Baseline	Definition
$\Omega_b h^2$	[0.005, 0.1]	–	Baryon density today
$\Omega_c h^2$	[0.001, 0.99]	–	Cold dark matter density today
$100\theta_{MC}$	[0.5, 10.0]	–	Sound horizon parameter(CosmoMC)
τ	[0.01, 0.8]	–	Thomson scattering optical depth of reionization
n_s	[0.9, 1.1]	–	Scalar spectrum power-law index
$\ln(10^{10} A_s)$	[2.7, 4.0]	–	Amplitude of primordial curvature perturbations
Σm_ν [eV]	[0, 5]	–	The sum of neutrino masses in eV
N_{eff}	[0.05, 10.0]	3.046	Effective number of neutrino-like relativistic degrees of freedom
w	[−3.0, −0.3]	−1	Dark energy equation of state
Ω_K	[−0.3, 0.3]	0	Curvature parameter today
A_L	[0, 10]	1	Normalized lensing spectrum amplitude

2 Data and methodology

The total *Planck* CMB temperature power-spectrum likelihood is divided into low- l ($l < 50$) and high- l ($l \geq 50$) parts. This is because the central limit theorem ensures that the distribution of CMB angular power spectrum C_l in the high- l regime can be well approximated by Gaussian statistics. However, for the low- l part the C_l distribution is non-Gaussian. For this reason the *Planck* team adopts two different methodologies to build the likelihood. In detail, for the low- l part, the likelihood exploits all *Planck* frequency channels from 30 to 353 GHz, separating the cosmological CMB signal from diffuse Galactic foregrounds through a physically motivated Bayesian component separation technique. For the high- l part, the *Planck* team employs a correlated Gaussian likelihood approximation, based on a fine-grained

set of angular cross-spectra derived from multiple detector combination between the 100, 143, and 217 GHz frequency channels, marginalizing over power-spectrum foreground templates. In order to break the well-known parameter degeneracy between the reionization optical depth τ and the scalar spectral index n_s , the *Planck* team adopts the low- l WMAP polarization likelihood (WP).

As stated above in this paper we are also interested in the X-ray cluster data [22–24]. The *CCCP* project measures cluster mass function by using a high-redshift ($0.4 < z < 0.9$) subsample of the 400 square degree survey, 37 objects, and low-redshift ($z < 0.2$) subsample of the all-sky survey, 49 brightest clusters. The methodologies of likelihood construction follow the standard derivation of the Poisson distribution of cluster mass [25]. The likelihood function implicitly depends on the cosmological parameters through the model of cluster mass function (reflecting the growth, normalization, and shape of the density perturbation power spectrum), through the cosmological volume-redshift relation which determines the survey volume, and through the distance-redshift as well as the masses-temperature relation. The details of likelihood construction and systematic uncertainty control are mentioned in [22]. Furthermore, in order to break the parameter degeneracies we also use some other external data sets, including BAO measurements from the 6dFGS [5], SDSS DR7 [6] and BOSS DR9 [7] surveys, and HST Key project [3] H_0 measurement.

Contrary to the *Planck* constraints on the summed neutrino mass, [11] found that adding X-ray cluster could give the non-zero detection of the active or sterile neutrino mass ($\sum m_\nu$ or m_s) with great statistical significance for various 8-parameter models, including the active/sterile neutrino mass as well as effective neutrino number N_{eff} . Moreover, adding X-ray data set could also lead to a significant deviation in σ_8 , namely the matter power spectrum amplitude on the $8h^{-1}\text{Mpc}$ scale, from the *Planck* result [2]. In details, without X-ray cluster, the *Planck* result favors a larger value of σ_8 , while with them the joint analysis give a lower value. Therefore, in this paper we explore the tension between *Planck* and *CCCP* X-ray cluster data sets with several 8-parameter models, including effective neutrino number N_{eff} , constant dark energy equation of state w , present spatial curvature Ω_K and lensing amplitude A_L . Particularly, we here focus on the neutrino mass constraint, so that in our baseline model the summed neutrino mass is always allowed to vary freely. We restrict ourselves to one-parameter extensions to the baseline model of $\Lambda\text{CDM} + \sum m_\nu$, as listed in Tab.1.

We compute the CMB angular and matter power spectra by using the public Einstein-Boltzmann solver *CAMB* [26] and explore the cosmological parameter space with a Markov Chain Monte Carlo sampler, namely *CosmoMC* [27]. For *Planck* we use the *Planck* Likelihood Code (PLC/clik) [28] which are available at the Planck Legacy Archive [29], and for *CCCP* our analysis is based on the likelihood grids presented in [22], which can be download from the website [30].

3 Results

In this section we will dig the information hidden in the *CCCP* X-ray cluster data [22–24]. Hereafter, we denote $CL_{X\text{-ray}}$ for this data. We will first investigate the constraints on the summed neutrino mass from the *Planck*+WP+BAO+HST data and $CL_{X\text{-ray}}$. Hereafter, we dub *Planck*+WP+BAO+HST as PWBH. Then, we will turn to reveal some tensions in some cosmological parameters between these two data sets.

Table 2. *Planck*+WP+BAO+HST+ $CL_{X\text{-ray}}$ results

Model	$\Lambda\text{CDM}+\Sigma m_\nu+N_{\text{eff}}$		$w\text{CDM}+\Sigma m_\nu$		$\Lambda\text{CDM}+\Sigma m_\nu+\Omega_K$	
	best fit	68% limits	best fit	68% limits	best fit	68% limits
$100\Omega_b h^2$	2.285	2.274 ± 0.027	2.205	2.204 ± 0.026	2.224	2.203 ± 0.031
$\Omega_c h^2$	0.1242	0.1227 ± 0.0044	0.1181	0.1176 ± 0.0016	0.1172	0.1179 ± 0.0026
$100\theta_{\text{MC}}$	1.04085	1.04092 ± 0.00070	1.04139	1.04125 ± 0.00057	1.04190	1.04125 ± 0.00065
τ	0.095	0.097 ± 0.015	0.086	0.090 ± 0.013	0.089	0.089 ± 0.013
n_s	0.9925	0.9929 ± 0.0098	0.9595	0.9621 ± 0.0059	0.9654	0.9624 ± 0.0077
$\ln(10^{10} A_s)$	3.107	3.109 ± 0.031	3.075	3.081 ± 0.025	3.083	3.080 ± 0.026
Σm_ν [eV]	0.47	0.46 ± 0.12	0.56	0.55 ± 0.10	0.41	0.45 ± 0.12
N_{eff}	3.80	3.704 ± 0.29	–	–	–	–
w	–	–	-1.39	-1.39 ± 0.12	–	–
Ω_K	–	–	–	–	0.00695	0.00835 ± 0.00411
Ω_m	0.2989	0.3000 ± 0.012	0.2693	0.2661 ± 0.0139	0.3027	0.3081 ± 0.0131
H_0	71.36	70.8 ± 1.5	73.68	74.0 ± 2.1	68.93	68.6 ± 1.0
σ_8	0.7461	0.7477 ± 0.0151	0.7902	0.7937 ± 0.0208	0.7434	0.7370 ± 0.0164
$\chi^2_{\text{min}}/2$	4911.581		4908.152		4912.452	

3.1 Σm_ν results

First, let us study the summed neutrino mass Σm_ν . The solar and atmospheric oscillation observations have already set a lower bound ($\Sigma m_\nu \geq 0.06$ eV) on the summed mass for the standard three neutrino species. Beside the local observations, we could also obtain neutrino mass information via the indirect measurements on the cosmological scales. Generally speaking, there are mainly two ways. One is through the secondary CMB anisotropies generated in the deep matter dominated epoch, such as weak lensing effect. However, these anisotropies are so small compared with the primordial signal that the current CMB experiments could only give a very loose upper bound, such as $\Sigma m_\nu < 0.66$ eV [2] from *Planck* [1]+ACT [31]+SPT [32–34]. The other method is to utilize the large scale structure tracers, such as matter power spectrum, selected cluster counting and cosmic shear, *etc.* Compared with the bounds obtained by CMB observations, these tomographic measurements could set a relatively stringent constraint. However, due to the contaminations from systematic noise and theoretical non-linearity *etc.*, the resulting constraint varies a lot among different projects. For example, $CL_{X\text{-ray}}$ [11] and selected Sunyaev-Zel’dovich galaxy cluster counts from *Planck* [14, 35] and SPT [36] report the non-zero detection of summed neutrino mass with quite significant evidence, while other galaxy surveys, such as WiggleZ [37] could improve the upper bound a lot but do not find any significant deviation from zero.

Given the above facts, in what follows we will use $CL_{X\text{-ray}}$ data to do the joint analysis of the summed neutrino mass Σm_ν with several related parameters, such as effective neutrino number N_{eff} , dark energy equation of state w as well as spatial curvature Ω_K . The results with or without $CL_{X\text{-ray}}$ are listed in Tab.2 or Tab.3. And the corresponding 2D likelihood contours are shown in Fig.1.

We summarise our main results in what follows. First of all, from Tab.2 one could find a more than 3σ detection of the summed neutrino mass for these three non-vanilla models

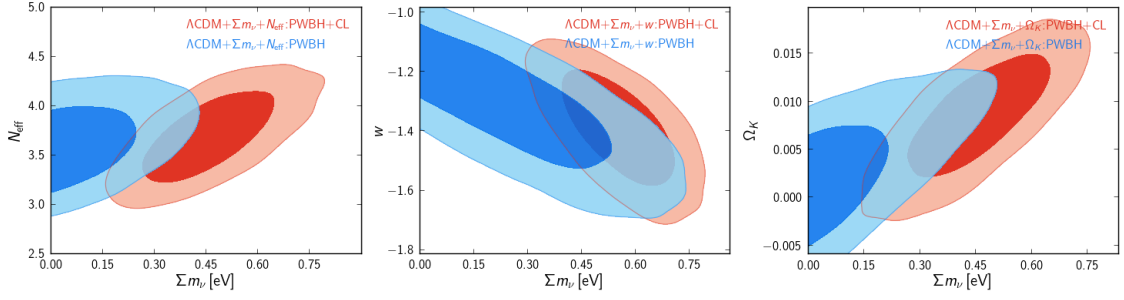


Figure 1. *Left:* Likelihood contours (68% CL and 95% CL) in the Σm_ν - N_{eff} plane for the $Planck+WP+BAO+H_0+CL_{X\text{-ray}}$ (red) and $Planck+WP+BAO+H_0$ (blue) data combinations. *Mid-* *dle:* Σm_ν - w likelihood contours. *Right:* Σm_ν - Ω_K likelihood contours.

Table 3. *Planck*+WP+BAO+HST results

Model	$\Lambda\text{CDM}+\Sigma m_\nu+N_{\text{eff}}$		$w\text{CDM}+\Sigma m_\nu$		$\Lambda\text{CDM}+\Sigma m_\nu+\Omega_K$	
	best fit	68% limits	best fit	68% limits	best fit	68% limits
$100\Omega_b h^2$	2.225	2.249 ± 0.027	2.183	2.193 ± 0.026	2.214	2.210 ± 0.031
$\Omega_c h^2$	0.1241	0.1275 ± 0.0048	0.1225	0.1209 ± 0.0022	0.1188	0.1192 ± 0.0028
$100\theta_{\text{MC}}$	1.04090	1.04060 ± 0.00071	1.04050	1.04105 ± 0.00059	1.04137	1.04138 ± 0.00066
τ	0.091	0.097 ± 0.014	0.086	0.089 ± 0.013	0.092	0.091 ± 0.013
n_s	0.9743	0.9830 ± 0.0097	0.9552	0.9571 ± 0.0065	0.9628	0.9619 ± 0.0077
$\ln(10^{10} A_s)$	3.102	3.122 ± 0.030	3.087	3.090 ± 0.025	3.092	3.091 ± 0.025
Σm_ν [eV]	0.039	< 0.34 (95% CL)	0.17	< 0.61 (95% CL)	0.018	< 0.38 (95% CL)
N_{eff}	3.44	3.661 ± 0.27	—	—	—	—
w	—	—	-1.27	-1.33 ± 0.15	—	—
Ω_K	—	—	—	—	0.0013	0.00318 ± 0.00415
Ω_m	0.2948	0.2986 ± 0.011	0.2778	0.2693 ± 0.0150	0.2978	0.3031 ± 0.0112
H_0	70.57	71.2 ± 1.5	72.53	73.7 ± 2.3	68.84	68.6 ± 1.0
σ_8	0.8463	0.8403 ± 0.0271	0.8828	0.8612 ± 0.0388	0.8384	0.8164 ± 0.0285
$\chi^2_{\text{min}}/2$	4903.787		4903.607		4905.298	

when $CL_{X\text{-ray}}$ data are taken into account

$$\Sigma m_\nu = 0.46 \pm 0.12 \text{ (68\% ; } + N_{\text{eff}} : \text{PWBH} + CL) , \quad (3.1)$$

$$\Sigma m_\nu = 0.55 \pm 0.10 \text{ (68\% ; } + w : \text{PWBH} + CL) , \quad (3.2)$$

$$\Sigma m_\nu = 0.45 \pm 0.12 \text{ (68\% ; } + \Omega_K : \text{PWBH} + CL) . \quad (3.3)$$

Moreover, as pointed out in [24] there exists a systematical error in hydrostatic mass measurements $\delta M/M \simeq 0.09$ in $CL_{X\text{-ray}}$ data sets. So, we take this mass function correction into account and list the corresponding results in Tab.4. Thanks to this correction, the mean value of summed neutrino mass get reduced

$$\Sigma m_\nu = 0.39 \pm 0.09 \text{ (68\% ; } + w : \text{PWBH} + CL + 9\% \text{Mass}). \quad (3.4)$$

3.2 A_L and σ_8 results

Then we study models including A_L and σ_8 , in which the latter is considered as a derived parameter from primordial curvature perturbation amplitude. Let us first investigate param-

Table 4. *Planck*+WP+BAO+HST+ $CL_{X-\text{RAY}}$ +9% Mass result

Model	$w\text{CDM}+\Sigma m_\nu$		$w\text{CDM}+\Sigma m_\nu+A_L$	
	best fit	68% limits	best fit	68% limits
$100\Omega_b h^2$	2.213	2.214 ± 0.024	2.226	2.243 ± 0.027
$\Omega_c h^2$	0.1178	0.1170 ± 0.0013	0.1182	0.1166 ± 0.0014
100θ	1.04175	1.04143 ± 0.00056	1.04129	1.04165 ± 0.00059
τ	0.086	0.089 ± 0.013	0.081	0.087 ± 0.013
n_s	0.9656	0.9648 ± 0.0054	0.9665	0.9685 ± 0.0057
$\ln(10^{10} A_s)$	3.077	3.080 ± 0.025	3.069	3.076 ± 0.024
Σm_ν [eV]	0.40	0.39 ± 0.09	0.42	0.38 ± 0.09
A_L	–	–	1.22	1.28 ± 0.10
w	–1.28	-1.23 ± 0.057	–1.29	-1.20 ± 0.07
Ω_m	0.2687	0.2766 ± 0.0113	0.2726	0.2780 ± 0.0118
H_0	73.26	72.0 ± 1.3	72.93	71.8 ± 1.5
σ_8	0.8109	0.7977 ± 0.0170	0.8031	0.7639 ± 0.0198
$\chi^2_{\min}/2$	4907.444		4903.368	

Table 5. CMB lensing amplitude A_L results

Model	$\Lambda\text{CDM}+\Sigma m_\nu+A_L$		$\Lambda\text{CDM}+A_L$		$\Lambda\text{CDM}+A_L$ (without HST+ $CL_{X-\text{ray}}$)	
	best fit	68% limits	best fit	68% limits	best fit	68% limits
$100\Omega_b h^2$	2.292	2.276 ± 0.027	2.304	2.285 ± 0.025	2.254	2.250 ± 0.028
$\Omega_c h^2$	0.1132	0.1131 ± 0.0011	0.1125	0.1124 ± 0.0010	0.1167	0.1166 ± 0.0017
$100\theta_{\text{MC}}$	1.04279	1.04224 ± 0.00056	1.04202	1.04224 ± 0.00056	1.04156	1.04186 ± 0.00058
τ	0.086	0.087 ± 0.013	0.075	0.073 ± 0.011	0.092	0.087 ± 0.013
n_s	0.9763	0.9768 ± 0.0053	0.9807	0.9784 ± 0.0051	0.9703	0.9698 ± 0.0059
$\ln(10^{10} A_s)$	3.069	3.068 ± 0.025	3.046	3.039 ± 0.021	3.091	3.078 ± 0.025
Σm_ν [eV]	0.25	0.28 ± 0.08	–	–	–	–
A_L	1.42	1.36 ± 0.10	1.44	1.37 ± 0.11	1.24	1.22 ± 0.10
Ω_m	0.2907	0.2942 ± 0.0108	0.2696	0.2693 ± 0.0057	0.2940	0.2929 ± 0.0099
H_0	69.12	68.7 ± 0.9	71.09	71.0 ± 0.5	68.97	69.1 ± 0.8
σ_8	0.7538	0.7550 ± 0.0139	0.7894	0.7867 ± 0.0070	0.8218	0.8162 ± 0.0119
$\chi^2_{\min}/2$	4907.083		4910.408		4903.236	

eter degeneracies. As shown in Fig.2, there exists only a tiny correlation between Σm_ν and A_L , so that the constraint on A_L in $\Lambda\text{CDM}+\Sigma m_\nu+A_L$ and $\Lambda\text{CDM}+A_L$ models are very close (see Tab.5). For example, using PWBH+ $CL_{X-\text{ray}}$ we could get

$$A_L = 1.37 \pm 0.11 \text{ (68\% ; } \Lambda\text{CDM} + A_L : \text{PWBH} + CL) . \quad (3.5)$$

Furthermore, we list the results of $\Lambda\text{CDM}+A_L$ model without $CL_{X-\text{ray}}$ in the third column of Tab.5 for comparison, which is well consistent with the *Planck* results [2]. It shows that without $CL_{X-\text{ray}}$ ¹

$$A_L = 1.22 \pm 0.10 \text{ (68\% ; } \Lambda\text{CDM} + A_L : \text{PWB}) . \quad (3.6)$$

Comparing (3.5) with (3.6) we could find that $CL_{X-\text{ray}}$ leads the A_L deviation from unity, the value in vanilla model, even larger. Moreover, in the second column of Tab.4, we can

¹In order to compare with the *Planck* results [2] we also remove HST data. As a background geometric measurements, HST data sets should be nearly blind to dynamical structure formation information on perturbation level. Hence, we should expect no significant change in A_L value after removing HST data.

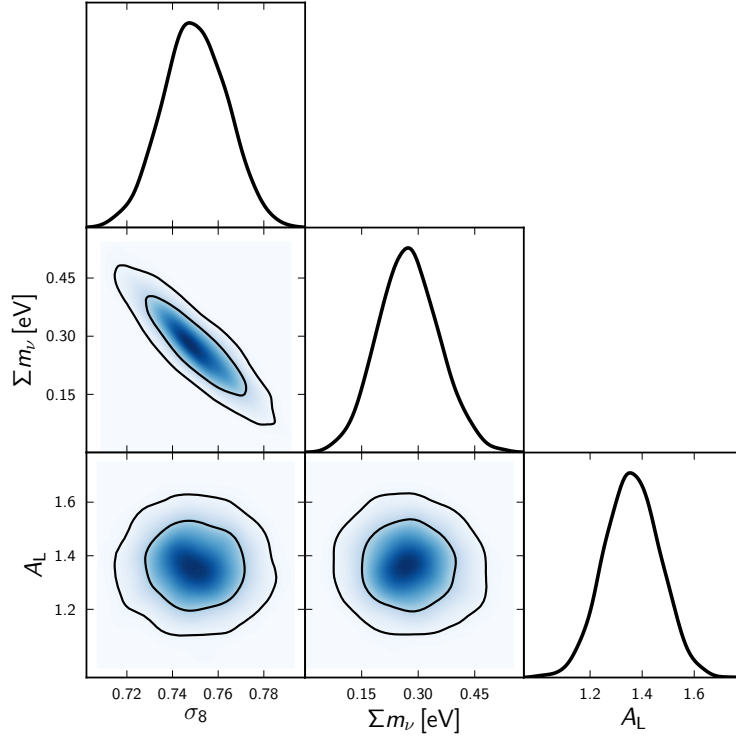


Figure 2. Triangle likelihood contours of σ_8 , $\sum m_\nu$ and A_L with *Planck*+WP+BAO+HST+ $CL_{X\text{-ray}}$.

see that by adding 9% mass correction, the tension in (3.5) with the vanilla model could be mildly reconciled

$$A_L = 1.28 \pm 0.10 \text{ (68\% ; } w\text{CDM} + \sum m_\nu + A_L : \text{PWBH} + CL + 9\%\text{Mass}) . \quad (3.7)$$

Then, we turn to the matter power spectrum amplitude σ_8 . As shown in Fig.2, there exists a significant anti-correlation between σ_8 and $\sum m_\nu$. This is because that the non-relativistic, massive, weakly-interacting neutrinos behave qualitatively as a species of warm/hot dark matter, suppressing fluctuations on scales smaller than their thermal free-streaming length. Consequently, this correlation will lead to a relatively low value of σ_8 when $\sum m_\nu$ is allowed to vary (see Fig.3 and Tab.5). For example, by using data sets PWBH+ $CL_{X\text{-ray}}$ our results give

$$\sigma_8 = 0.7894 \pm 0.0070 \text{ (68\% ; } \Lambda\text{CDM} + A_L : \text{PWBH} + CL) , \quad (3.8)$$

$$\sigma_8 = 0.7550 \pm 0.0139 \text{ (68\% ; } \Lambda\text{CDM} + \sum m_\nu + A_L : \text{PWBH} + CL) . \quad (3.9)$$

In 6 parameter Λ CDM model, *Planck* collaboration [35] gives $\sigma_8(\Omega_m/0.27)^{0.3} = 0.784 \pm 0.027$ by using *Planck*+WP+BAO+BBN+ $CL_{X\text{-ray}}$, which is consistent with the results reported here. We notice that in Fig.3 the results with $CL_{X\text{-ray}}$ (3.9) (blue curve) are in a 2σ tension with those in absence of $CL_{X\text{-ray}}$ data (3.10) (red curve)

$$\sigma_8 = 0.8162 \pm 0.0119 \text{ (68\% ; } \Lambda\text{CDM} + A_L : \text{PWB}) . \quad (3.10)$$

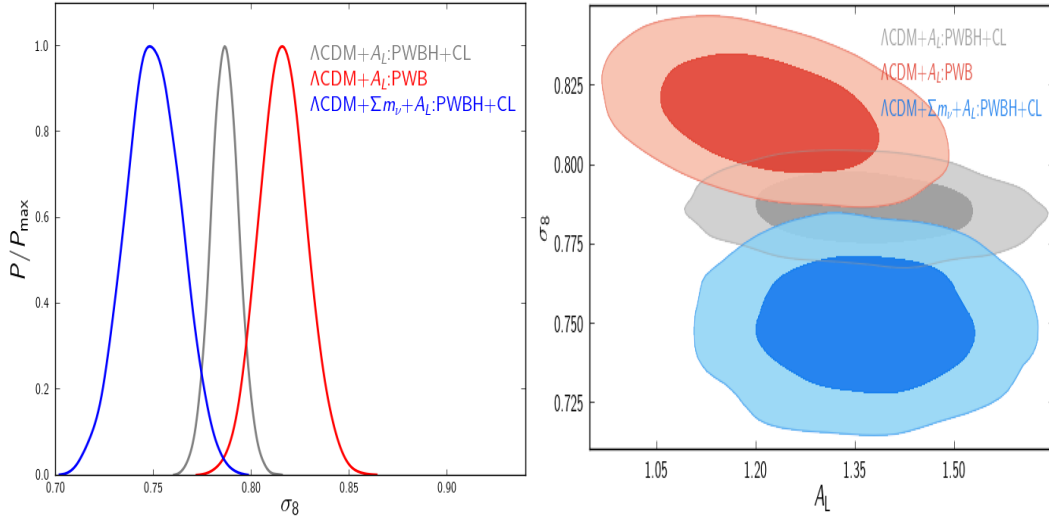


Figure 3. *Left:* Marginalized likelihoods of σ_8 . *Right:* 2D likelihood contours between the lensing amplitude A_L and rms amplitude of linear fluctuation σ_8 .

Similar to A_L , with a 9% cluster mass correction we could also reconcile the tension with *Planck*

$$\sigma_8 = 0.7639 \pm 0.0198 \text{ (68\% ; } w\text{CDM} + \sum m_\nu + A_L : \text{PWBH} + CL + 9\%\text{Mass}) . \quad (3.11)$$

3.3 H_0 and w results

In this subsection, we study two background parameters, Hubble constant H_0 and Dark Energy (DE) Equation of State (EoS) w .

First of all, we can see from Tab.2 that without 9% mass correction to $CL_{X\text{-ray}}$ data sets, a larger H_0 value is favored, e.g. for $w\text{CDM}+\sum m_\nu$ model:

$$H_0 = 74.0 \pm 2.1 \text{ (68\% ; } +w : \text{PWBH} + CL) . \quad (3.12)$$

However, after adding this corrections one could pull the mean value of H_0 a little bit back for the same model

$$H_0 = 72.0 \pm 1.3 \text{ (68\% ; } +w : \text{PWBH} + CL + 9\%\text{Mass}) . \quad (3.13)$$

Second, instead of the spatial curvature Ω_K , once DE EoS w is treated as a free parameter, a larger H_0 arrives (see the left panel of Fig.4). This is due to the $H_0 - w$ correlation illustrated in the right panel of Fig.4. Third, for a consistency check we also include the results from joint analysis of WMAP7 and $CL_{X\text{-ray}}$ data. The right panel of Fig.4 clearly shows that there exists a 2σ tension in the parameter plane between the *Planck*+WP+BAO+HST+ $CL_{X\text{-ray}}$ (blue) and WMAP7+BAO+HST+ $CL_{X\text{-ray}}$ (green) data.

Beside the above H_0 discrepancies, we also notice that a phantom-like DE EoS [38] is favored in our results

$$w = -1.39 \pm 0.12 \text{ (68\% ; } +w : \text{PWBH} + CL) . \quad (3.14)$$

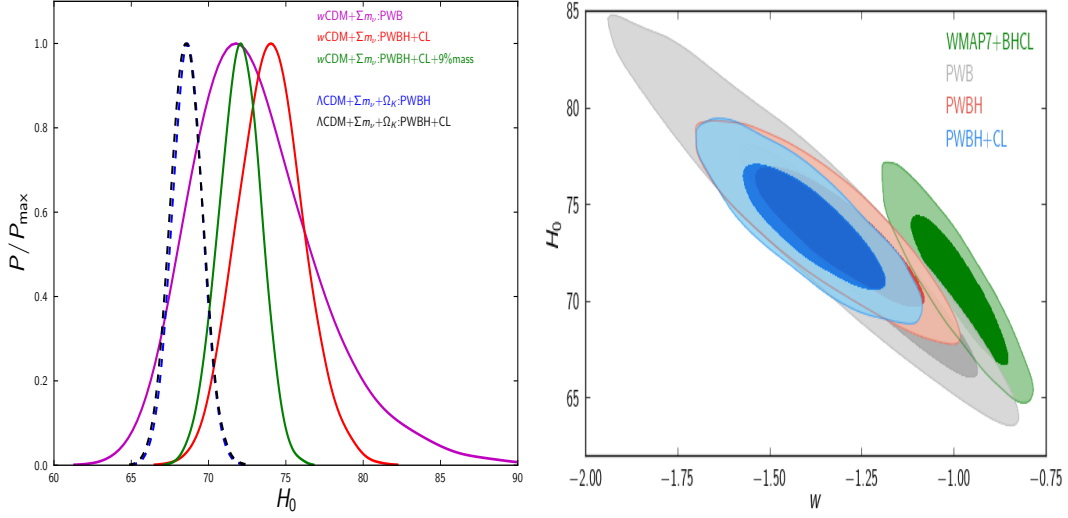


Figure 4. *Left:* marginalized likelihood of H_0 for w CDM+ Σm_ν (solid) and Λ CDM+ $\Sigma m_\nu + \Omega_K$ (dashed) model. *Right:* 2D likelihood contours in the $H_0 - w$ plane.

However, we should emphasize that this phantom-like value of DE EoS is not resulted in by including $CL_{X\text{-ray}}$ data. From the middle column of Tab.3, one can find that without X-ray cluster data the DE EoS still deviates from -1 more than 2σ confidence level

$$w = -1.33 \pm 0.15 \text{ (68\% ; } +w : \text{PWBH)}. \quad (3.15)$$

Furthermore, if we also remove HST data, i.e. just use *Planck*+WP+BAO, there will be no significant deviation from $w = -1$ as

$$w = -1.31 \pm 0.23 \text{ (68\% ; } +w : \text{PWB)}. \quad (3.16)$$

Because of the well-known $H_0 - w$ correlation, we argue that this result partially reflects the tension between HST and *Planck* on Hubble parameter H_0 as found in [2]. At last, the 9% mass correction can also relax the tension in w with Λ CDM model

$$w = -1.23 \pm 0.06 \text{ (68\% ; } +w : \text{PWBH} + CL + 9\% \text{Mass)}. \quad (3.17)$$

4 Conclusions

We have presented an updated estimation of cosmological parameters in three 8-parameter non-vanilla models using *Planck* WMAP7, BAO, HST and *CCCP* X-ray data sets. First of all, we have found that X-ray cluster data sets strongly favor a non-zero summed neutrino mass with more than 3σ CL in these models, which is in quite good agreement with recent results in the literature. The presence of massive neutrinos inhibits the growth of structures below their thermal free-streaming scale during structure formation, leading to a reduced value of σ_8 , which could improve consistency with X-ray cluster data. In addition, we have also revealed some tensions between X-ray cluster and *Planck* data in the cosmological parameters, including the matter power spectrum amplitude σ_8 , lensing amplitude A_L , constant dark energy equation of state w as well as Hubble parameter H_0 .

For the matter power spectrum amplitude σ_8 , X-ray cluster data favor a relatively low value compared with *Planck*. Because of the $\sigma_8 - \sum m_\nu$ degeneracy, this tension could be beyond 2σ CL when the summed neutrino mass $\sum m_\nu$ is allowed to vary. For the CMB lensing amplitude A_L , the addition of X-ray cluster data makes its deviation from unity (vanilla model) even worse and results in more than 3σ discrepancy. Because of the correlation between H_0 and w , X-ray cluster data prefer a large Hubble constant and quite negative dark energy equation of state. Furthermore, we have also found a 2σ tension in the $H_0 - w$ plane between the *Planck*+WP+BAO+HST+ $CL_{X\text{-ray}}$ and WMAP7+BAO+HST+ $CL_{X\text{-ray}}$ data. Finally, we should emphasize that these tensions/discrepancies could be reduced in some sense by making a 9% shift in the cluster mass functions. The resolution of these tensions will likely require either the identification of a currently-unknown systematic effect in at least one of these data sets or new physics.

Acknowledgments

This work is partially supported by the project of Knowledge Innovation Program of Chinese Academy of Science, NSFC under Grant No.11175225, No.11335012, and National Basic Research Program of China under Grant No.2010CB832805 and No.2010CB833004. BH is supported by the Dutch Foundation for Fundamental Research on Matter (FOM).

References

- [1] P. A. R. Ade *et al.* [Planck Collaboration], arXiv:1303.5062 [astro-ph.CO].
- [2] P. A. R. Ade *et al.* [Planck Collaboration], arXiv:1303.5076 [astro-ph.CO].
- [3] W. L. Freedman *et al.* [HST Collaboration], *Astrophys. J.* **553**, 47 (2001) [astro-ph/0012376].
- [4] N. Suzuki, D. Rubin, C. Lidman, G. Aldering, R. Amanullah, K. Barbary, L. F. Barrientos and J. Botyanszki *et al.*, *Astrophys. J.* **746**, 85 (2012) [arXiv:1105.3470 [astro-ph.CO]].
- [5] F. Beutler, C. Blake, M. Colless, D. H. Jones, L. Staveley-Smith, L. Campbell, Q. Parker and W. Saunders *et al.*, *Mon. Not. Roy. Astron. Soc.* **416**, 3017 (2011) [arXiv:1106.3366 [astro-ph.CO]].
- [6] W. J. Percival *et al.* [SDSS Collaboration], *Mon. Not. Roy. Astron. Soc.* **401**, 2148 (2010) [arXiv:0907.1660 [astro-ph.CO]].
- [7] L. Anderson, E. Aubourg, S. Bailey, D. Bizyaev, M. Blanton, A. S. Bolton, J. Brinkmann and J. R. Brownstein *et al.*, *Mon. Not. Roy. Astron. Soc.* **427**, no. 4, 3435 (2013) [arXiv:1203.6594 [astro-ph.CO]].
- [8] C. Cheng and Q. -G. Huang, arXiv:1306.4091 [astro-ph.CO].
- [9] B. Hu, M. Liguori, N. Bartolo and S. Matarrese, arXiv:1307.5276 [astro-ph.CO].
- [10] A. Marchini and V. Salvatelli, *Phys. Rev. D* **88**, 027502 (2013) [arXiv:1307.2002 [astro-ph.CO]].
- [11] M. Wyman, D. H. Rudd, R. A. Vanderveld and W. Hu, arXiv:1307.7715 [astro-ph.CO].
- [12] J. -Q. Xia, H. Li and X. Zhang, *Phys. Rev. D* **88**, 063501 (2013) [arXiv:1308.0188 [astro-ph.CO]].
- [13] J. Hamann and J. Hasenkamp, *JCAP* **1310**, 044 (2013) [arXiv:1308.3255 [astro-ph.CO]].
- [14] R. A. Battye and A. Moss, arXiv:1308.5870 [astro-ph.CO].
- [15] Z. Li, P. Wu, H. Yu and Z. -H. Zhu, arXiv:1311.3467 [astro-ph.CO].

- [16] R. -G. Cai, Z. -K. Guo and B. Tang, arXiv:1312.4309 [astro-ph.CO].
- [17] A. Vikhlinin, A. Kravtsov, W. Forman, C. Jones, M. Markevitch, S. S. Murray and L. Van Speybroeck, *Astrophys. J.* **640**, 691 (2006) [astro-ph/0507092].
- [18] O. Kotov and A. Vikhlinin, *Astrophys. J.* **641**, 752 (2006) [astro-ph/0511044].
- [19] A. V. Kravtsov, A. Vikhlinin and D. Nagai, *Astrophys. J.* **650**, 128 (2006) [astro-ph/0603205].
- [20] D. Nagai, A. Vikhlinin and A. V. Kravtsov, *Astrophys. J.* **655**, 98 (2007) [astro-ph/0609247].
- [21] R. A. Burenin, A. Vikhlinin, A. Hornstrup, H. Ebeling, H. Quintana and A. Mescheryakov, [astro-ph/0610739].
- [22] A. Vikhlinin, R. A. Burenin, H. Ebeling, W. R. Forman, A. Hornstrup, C. Jones, A. V. Kravtsov and S. S. Murray *et al.*, *Astrophys. J.* **692**, 1033 (2009) [arXiv:0805.2207 [astro-ph]].
- [23] A. Vikhlinin, A. V. Kravtsov, R. A. Burenin, H. Ebeling, W. R. Forman, A. Hornstrup, C. Jones and S. S. Murray *et al.*, *Astrophys. J.* **692**, 1060 (2009) [arXiv:0812.2720 [astro-ph]].
- [24] R. A. Burenin and A. A. Vikhlinin, arXiv:1202.2889 [astro-ph.CO].
- [25] W. Cash, *Astrophys. J.* **228**, 939 (1979).
- [26] A. Lewis, A. Challinor and A. Lasenby, *Astrophys. J.* **538**, 473 (2000) [astro-ph/9911177].
- [27] A. Lewis and S. Bridle, *Phys. Rev. D* **66**, 103511 (2002) [astro-ph/0205436].
- [28] P. A. R. Ade *et al.* [Planck Collaboration], arXiv:1303.5075 [astro-ph.CO].
- [29] [http://www.sciops.esa.int/index.php?project=planck&page=Planck Legacy Archive](http://www.sciops.esa.int/index.php?project=planck&page=Planck%20Legacy%20Archive)
- [30] <http://hea.iki.rssi.ru/400d/cosm/>
- [31] S. Das, T. Louis, M. R. Nolta, G. E. Addison, E. S. Battistelli, J. R. Bond, E. Calabrese and D. C. M. J. Devlin *et al.*, arXiv:1301.1037 [astro-ph.CO].
- [32] R. Keisler, C. L. Reichardt, K. A. Aird, B. A. Benson, L. E. Bleem, J. E. Carlstrom, C. L. Chang and H. M. Cho *et al.*, *Astrophys. J.* **743**, 28 (2011) [arXiv:1105.3182 [astro-ph.CO]].
- [33] K. T. Story, C. L. Reichardt, Z. Hou, R. Keisler, K. A. Aird, B. A. Benson, L. E. Bleem and J. E. Carlstrom *et al.*, *Astrophys. J.* **779**, 86 (2013) [arXiv:1210.7231 [astro-ph.CO]].
- [34] C. L. Reichardt, L. Shaw, O. Zahn, K. A. Aird, B. A. Benson, L. E. Bleem, J. E. Carlstrom and C. L. Chang *et al.*, *Astrophys. J.* **755**, 70 (2012) [arXiv:1111.0932 [astro-ph.CO]].
- [35] P. A. R. Ade *et al.* [Planck Collaboration], arXiv:1303.5080 [astro-ph.CO].
- [36] Z. Hou, C. L. Reichardt, K. T. Story, B. Follin, R. Keisler, K. A. Aird, B. A. Benson and L. E. Bleem *et al.*, arXiv:1212.6267 [astro-ph.CO].
- [37] S. Riemer-Sørensen, D. Parkinson and T. M. Davis, arXiv:1306.4153 [astro-ph.CO].
- [38] R. R. Caldwell, *Phys. Lett. B* **545**, 23 (2002) [astro-ph/9908168].
- [39] D. Spergel, R. Flauger and R. Hlozek, arXiv:1312.3313 [astro-ph.CO].